NASA TR R-80

NATIONAL AERONAUTICS AND SPACE ADMINISTRATION

TECHNICAL REPORT
R-80

THE EFFECT OF LIFT ON ENTRY CORRIDOR DEPTH AND GUIDANCE REQUIREMENTS FOR THE RETURN LUNAR FLIGHT

By THOMAS J. WONG and ROBERT E. SLYE

1961

For sale by the Superintendent of Documents, U.S. Government Printing Office, Washington 25, D.C. Yearly subscription, $15; foreign, $19; single copy price varies according to size ..... Price 30 cents

TECHNICAL REPORT R-80

THE EFFECT OF LIFT ON ENTRY CORRIDOR DEPTH AND GUIDANCE REQUIREMENTS FOR THE RETURN LUNAR FLIGHT

By THOMAS J. WONG and ROBERT E. SLYE

Ames Research Center
Moffett Field, Calif.

TECHNICAL REPORT R-80

THE EFFECT OF LIFT ON ENTRY CORRIDOR DEPTH AND GUIDANCE REQUIREMENTS FOR THE RETURN LUNAR FLIGHT

By Thomas J. Wong and Robert E. Slye

SUMMARY

Entry corridors for manned vehicles returning from the moon are defined consistent with requirements for avoiding radiation exposure and for limiting values of peak deceleration. It was found that the use of lift increases the depth of the entry corridor and, hence, reduces guidance accuracy requirements. Mid-course guidance requirements appear to be critical only for the flight-path angle. Increasing the energy of the transfer orbit increases the required guidance accuracy for the flight-path angle.

To correct a trajectory for an error in target perigee point, it was found that application of the corrective thrust essentially parallel to the local horizontal produces the maximum change in perigee altitude for a given increment of velocity. It was also found that the energy required to effect a given change in perigee altitude is not strongly dependent on the energy of the orbit, but it was found to vary inversely with range measured from the center of the earth. For this reason, it is important to detect and correct any errors in approach trajectory at the largest possible distance from the earth.

INTRODUCTION

The use of multiple-graze trajectories for atmosphere entry has been studied in some detail as a possible method for alleviating the heating and deceleration problems encountered by manned space vehicles during entry (see refs. 1, 2, and 3). This type of trajectory, however, requires very precise control of the approach orbit (see ref. 4). Because of such severe guidance requirements, the multiple-graze type entry does not appear attractive at the present time. When allowances are made for finite guidance tolerances of single-graze entries, a vehicle will be required to operate through larger ranges of entry angles and altitudes and hence more severe decelerations and heating conditions than for multiple-graze type entries. Limiting values of deceleration and heating will determine a flight corridor through which the vehicle must fly for successful entry. The depth of the corridor then determines the allowable tolerances on the velocity vector. Some of these problems for a circumnavigating lunar vehicle were presented by Xenakis in reference 5 in which calculations were made for ballistic vehicles only. The purpose of the present paper is to determine the effect of lift on the entry corridor and guidance requirements for the return lunar flight. A similar analysis of entries into other planetary atmospheres as well as entries into earth's atmosphere following return from interplanetary space is presented by Chapman in reference 6. Guidance requirements for entry into earth's atmosphere, however, were evaluated only for vehicles having lift-drag ratios of unity and parabolic approach orbits.

GENERAL CONSIDERATIONS

EFFECT OF RADIATION BELTS

In addition to the guidance considerations just discussed, the high-intensity radiation belts discovered through the IGY sponsored experiments of Van Allen (see, e.g., ref. 7) also impose some restrictions on the flight of manned space vehicles. It is indicated, for instance, that manned satellites should be restricted to orbiting altitudes below 400 miles or above 30,000 miles. Van Allen has also speculated that manned space vehicles may best

leave and approach the earth through the radiation-free zones over the poles (ref. 7). The presence of these belts imposes further restrictions on the entry procedure. For example, if a vehicle approaching the earth makes a light graze of the atmosphere, losing only a small portion of its velocity in the first graze, several grazes are required before the velocity is reduced sufficiently for the vehicle to make its final descent. The use of a weak initial graze would not only be uneconomical of time, but it would also cause the vehicle to make several passes through the high-intensity radiation belts as shown by the dashed line in figure 1. In order to avoid the radiation belts, the vehicle should enter on a sufficiently low trajectory (represented by the solid line in fig. 1) that entry may be completed in the first pass, or if the vehicle leaves the atmosphere, the apogee altitude following exit should not exceed about 400 miles.

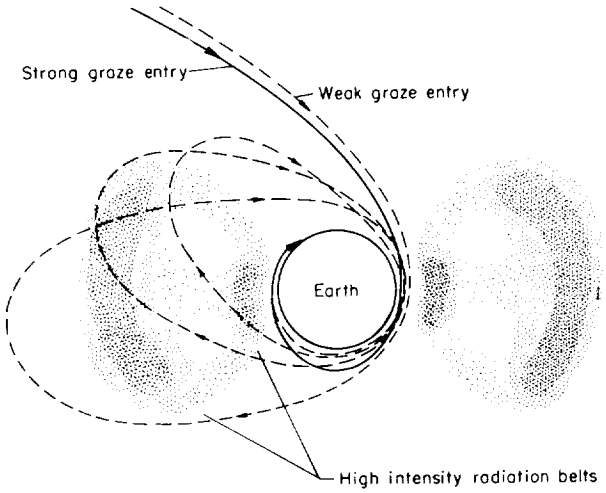

FIGURE 1.—Grazing entries.

ENTRY CORRIDOR

Manned vehicles must also be restricted to entry trajectories which are characterized by limited decelerations and small entry angles. These restrictions and those imposed by the radiation belts may be used to define an entrance corridor for a vehicle. Typical corridor boundaries are shown in figure 2. Consider first the entry corridor of the ballistic vehicle as shown in figure 2(a). Overshoot boundaries may be defined consistent

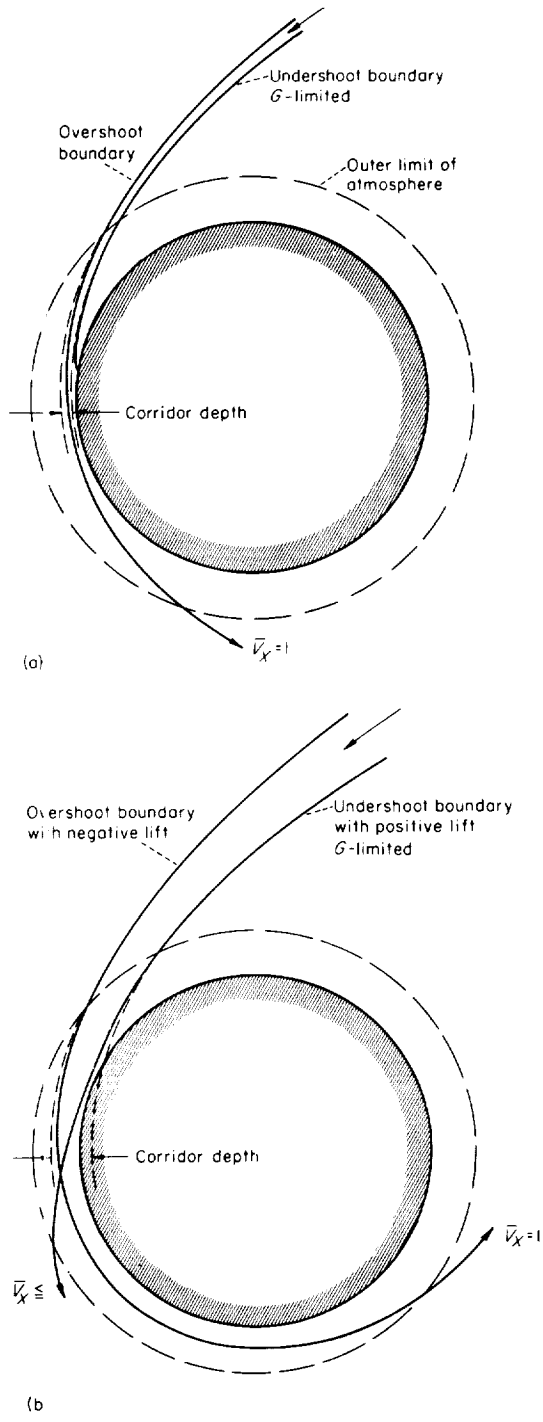

(a) Ballistic corridor.
(b) Lifting corridor.

FIGURE 2.—Entrance corridors.

with the restrictions of the radiation belts by limiting the highest approach to that for which a vehicle may exit the atmosphere with local circular satellite speed. For a ballistic vehicle, such an exit is possible only at the upper boundary of the corridor. A lower approach would lead to higher decelerations and entry would be completed in the first pass. Lower or undershoot boundaries may be defined by the lowest trajectory for which the vehicle would encounter a peak deceleration not exceeding an acceptable value. Above the corridor the vehicle would enter a multiple-graze type trajectory and encounter radiation hazards or, if the entry trajectory were sufficiently high, no reduction in velocity would occur and the vehicle would remain on its original orbit. Below the corridor the vehicle would encounter hazardous decelerations. The entry corridor is then represented by the area between the limiting trajectories (solid lines) outside the atmosphere and their "vacuum" extensions (dotted lines representing the trajectory that would have occurred if the atmosphere had not altered the path of the vehicle) inside the atmosphere.

The corridor depth may be increased by use of lift as indicated in figure 2(b). At the overshoot boundary a higher approach than for the ballistic vehicle may be made because negative lift can be used to hold the vehicle in the atmosphere thus resulting in lower decelerations occurring over a longer period of time. At the undershoot boundary, positive lift turns the vehicle upward and away from the vacuum trajectory. At a given peak deceleration, a lifting vehicle with a small L/D and a ballistic vehicle with the same m/C_DA are approximately at the same altitude. It is apparent that for equal G's, a lifting vehicle will enter the atmosphere at steeper angles, and, therefore, its approach trajectory is lower than that for the ballistic vehicle. Use of lift then increases the corridor depth by extending both the overshoot and undershoot boundaries.

The depth of the entry corridor may of course be measured at any point along a mean trajectory. However, at any point other than apogee or perigee of the vacuum trajectory, the flight-path angle is different from zero and the definition of the corridor would not only require a specification of a depth but also a range of allowable flight-path angles. For convenience, then, the corridor depth is taken as the difference in perigee altitudes of the vacuum trajectories. The technique of using differences in perigee altitudes as a measure of entry corridors for determining guidance requirements for circumlunar flights was also used by Lieske (ref. 8), Xenakis (ref. 5), and in a more general and recent study by Chapman (ref. 6).

ANALYSIS

CORRIDOR DEPTH

In calculating the corridor depth, it will be convenient to first derive an approximate equation relating the vacuum perigee radius to entrance conditions. For the return trip from the moon, the velocity at any point near perigee is sufficiently near the local escape speed that the trajectory near the earth may be approximated with a parabola (see sketch (a)). For a parabolic orbit,

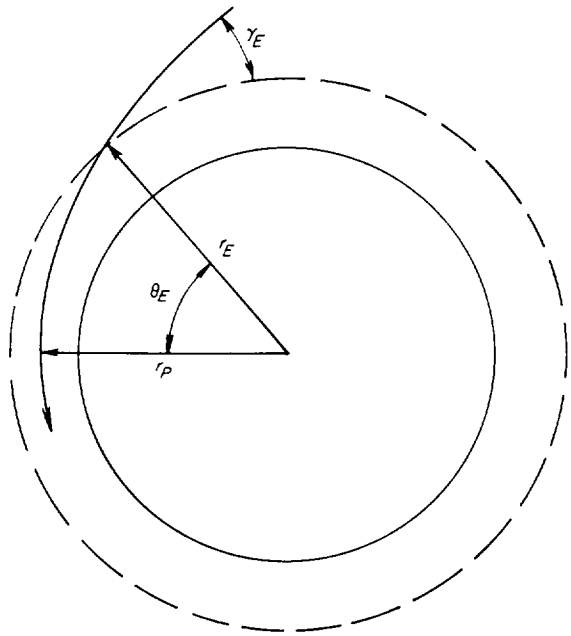

Sketch (a).

the perigee radius is related to the entrance radius and θ_E by

$$\frac{r_p}{r_E}=\frac{1+\cos\theta_E}{2} \tag{1}$$

The flight-path angle, γ, in this case is equal to $\theta/2$. (All symbols are defined in appendix A.)

Thus equation (1) in terms of the flight-path angle becomes

$$\frac{r_p}{r_E}=1-\sin^2\gamma_E \tag{2}$$

Noting that $r=r_o+y$ and for $y\ll r_o$ and $\gamma_E\ll 1$ the perigee altitude is given approximately by

$$y_p=y_E-r_o\gamma_E^2 \tag{3}$$

Below the entrance point in the actual trajectory, aerodynamic forces become important and the motion is approximately defined by the differential equation (ref. 1)

$$\left.\begin{aligned}&\frac{d^2f}{dZ^2}+\frac{I}{f}(1-e^{-Z})+J=0\\ &\text{where}\\ &f=e^{-\beta y}=\frac{\rho}{\rho_o\alpha}\\ &Z=\ln(V^2/gr_o)\\ &I=\frac{\beta}{r_o}\left(\frac{m}{C_DA\rho_o\alpha}\right)^2\\ &J=\frac{\sqrt{I\beta r_o}}{2}\frac{L}{D}\end{aligned}\right\} \tag{4}$$

The entrance altitude and flight-path angle in terms of the initial conditions for the solutions to equation (4) are

$$y_E=-\frac{1}{\beta}\ln f_E \tag{5}$$

and

$$\gamma_E=\frac{1}{\sqrt{I\beta r_o}}\left(\frac{df}{dZ}\right)_E \tag{6}$$

For convenience, let

$$F\equiv\frac{f}{\sqrt{I}}\quad\text{and}\quad F'\equiv\frac{1}{\sqrt{I}}\frac{df}{dZ} \tag{7}$$

With equations (5), (6), and (7), equation (3) becomes

$$\ln F_p=\ln F_E+(F_E')^2 \tag{8}$$

which relates the density at the vacuum perigee altitude to the entrance conditions for the solutions of equation (4). The perigee altitude in statute miles follows from equations (4) and (8); thus

$$y_p=-\frac{\ln F_p\sqrt{I}}{5280\,\beta}=-4.7\ln\frac{F_p}{\rho_o\alpha}\sqrt{\frac{\beta}{r_o}}\left(\frac{m}{C_DA}\right),\ \text{mi} \tag{9}$$

For trajectories in which entry is completed in a single pass, perigee parameters were determined from the initial conditions for solutions obtained by machine integration of equation (4). For trajectories in which the vehicle leaves the atmosphere with $\overline{V}_X=1$, the series solutions to equation (4), presented in appendix B, were employed. In all cases, perigee parameters were obtained for a range of entrance conditions. Cross plots of deceleration versus perigee parameters for given values of L/D were made and interpolated to obtain corridor parameters for given values of peak decelerations of 10, 15, and 20 g.

There were small differences in perigee altitudes between the machine and series solutions. However, changes in perigee altitude for given values of peak deceleration were approximately the same. The perigee altitude for $L/D=0$ and $\overline{V}_X=1$ was therefore taken from the machine solutions and changes in perigee altitude for $L/D\neq 0$ were determined from the series solutions.

The entry-corridor depth is simply the difference in perigee altitudes between the overshoot and undershoot trajectories, or

$$\Delta y_p=4.7\left(\ln\frac{F_{p_{\text{un}}}}{F_{p_{\text{ov}}}}+\ln\frac{C_{D_{\text{ov}}}}{C_{D_{\text{un}}}}\right),\ \text{mi} \tag{10}$$

It is apparent from equation (10) that if the drag coefficient is the same at both boundaries, the corridor depth will be independent of the drag-loading parameter, m/C_DA. The average altitude of the corridor, on the other hand, is dependent on the mass and drag characteristics of the vehicle (see eq. (9)). Likewise, the proportion of corridor depth obtainable with negative and with positive L/D for a given vehicle will depend on the variation of C_D with L/D and whether L/D is changed by decreasing or increasing C_D from the value used at the corridor boundaries.

HEATING IN THE CORRIDOR

Heating in the grazes was also obtained by the method of reference 1 which, for convenience, is also outlined in appendix B.

LANDING POINT

Due to the fact that the L/D in the first graze is dependent on the location of the vehicle in the flight corridor, the range traveled and, therefore, the landing point will also be dependent on the location of the vehicle in the corridor. In general, then, it will not be possible for nonlifting vehicles or vehicles with very small lift-drag ratios to land at any preselected point. For the trajectories in which the vehicle leaves the atmosphere with $\overline{V}_X=1$ and a sufficiently large flight-path angle, it is possible to convert the trajectory into a satellite orbit by applying a small amount of rocket thrust when the vehicle reaches apogee. It would then be possible to wait until the vehicle had orbited closer to the desired landing point before initiating the final descent. The maximum waiting time would be less than 12 hours.

For $\overline{V}_X=1$, the apogee radius is given by

$$r_a=r_X(1+\sin\gamma_X)=a(1+e) \tag{11}$$

where γ_X is the flight-path angle at exit and for the grazing trajectories considered, it will be very close to $-(2/3)\gamma_E$ (see eqs. (B9) and (B10)). It is apparent from equation (11) that r_X is the semimajor axis and sin γ_X is the eccentricity of the orbit. For conversion to a circular orbit, the velocity increment to be provided by rocket thrust is simply the difference between the local circular satellite speed and the velocity at apogee, or

$$\Delta V=\sqrt{\frac{\mu}{r_a}}\left(1-\sqrt{1-\sin\gamma_X}\right) \tag{12}$$

which for, $\gamma_X\ll 1$, is given approximately by

$$\Delta V=\frac{\gamma_X}{2}\sqrt{\frac{\mu}{r_a}} \tag{13}$$

If apogee is much greater than 100 miles, conversion to a circular orbit may provide more orbit lifetime than is required for a 12-hour waiting period and thus would be uneconomical of rocket fuel. In this case raising perigee to, say, 100 miles may be all that is required for a 12-hour waiting period. The eccentricity of this orbit would be

$$e=\frac{r_a-(r_o+100\times 5280)}{r_a+(r_o+100\times 5280)} \tag{14}$$

where r_o is the radius of the earth.

The velocity increment required at apogee is the difference in velocity of this orbit at apogee and that of the orbit following exit after the initial graze. For small eccentricities the velocity increment is given approximately by

$$\Delta V=\sqrt{\frac{\mu}{r_a}}\left(\frac{\gamma_X-e}{2}\right) \tag{15}$$

Let us consider next the development of equations to evaluate the guidance requirements for the return lunar flight.

GUIDANCE REQUIREMENTS

To assess the guidance requirements for the lunar return trip, it was assumed that the vehicle, after essentially leaving the moon's gravitational field ($r/r_m<0.9$), traveled along an elliptical orbit as shown in figure 3. The orbit was assumed to

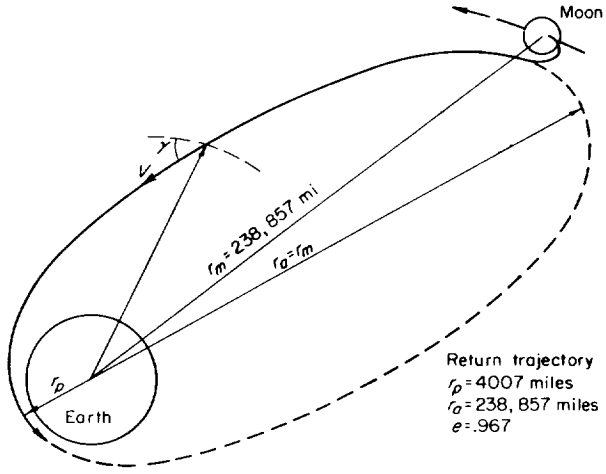

FIGURE 3.—Return trajectory.

have an apogee radius equal to the mean radius of the moon's orbit around the earth and a perigee altitude equal to 44 miles.[1] The eccentricity of this orbit is 0.967. A vehicle on such an orbit would require a transfer time of about 5 days from launch on the moon to its entry corridor. A slight increase in eccentricity will greatly reduce the transfer time. To assess, in part, the effect of transfer energy on guidance requirements, a study will also be made of orbits having eccentricities of 1.0 and 1.033. To evaluate the guidance accuracy requirements it will be convenient to obtain a single

[1] It will be seen later that 44 miles is the vacuum perigee altitude for a ballistic vehicle having an $m/C_DA=1$ slug/ft^2 and entering along the overshoot boundary of its corridor.

relation for the perigee radius as a function of r, V, and γ. The following equations for motion along an orbit described by a conic section were employed (see, e.g., ref. 9),

$$r=\frac{a(1-e^2)}{1+e\cos\theta}=\frac{r_p(1+e)}{1+e\cos\theta} \tag{16}$$

$$V^2=\mu\left(\frac{2}{r}-\frac{1}{a}\right) \tag{17}$$

and

$$h=rV\cos\gamma=\text{constant}=r_pV_p \tag{18}$$

From these equations, the following relation for the perigee radius may be derived

$$r_p=\frac{r^2V^2\cos^2\gamma}{\mu(1+e)} \tag{19}$$

where

$$e=\sqrt{1-\frac{rV^2}{\mu}\left(2-\frac{rV^2}{\mu}\right)\cos^2\gamma}$$

By partial differentiation of equation (19), the derivatives obtained represent a first approximation of the error in perigee radius due to individual unit errors in r, V, or γ. These derivatives are as follows:

$$\frac{\partial r_p}{\partial r}=\frac{r_p}{r}\left(2+\frac{1-\overline{V}^2}{e}\frac{r_p}{r}\right) \tag{20}$$

$$\frac{\partial r_p}{\partial V}=\frac{2r_p}{eV}\left(1-\frac{r_p}{r}\right) \tag{21}$$

$$\frac{\partial r_p}{\partial\gamma}=-r_p\frac{1+e}{e}\tan\gamma \tag{22}$$

where

$$\tan\gamma=\sqrt{\frac{r/r_p}{1+e}\left[2-\frac{r}{r_p}(1-e)\right]-1}$$

Total errors in r_p due to small combined errors may be determined with the equation for the total differential; thus, for an orbit initially parabolic, we have

$$\frac{\Delta r_p}{r_p}=\left(2-\frac{r_p}{r}\right)\frac{\Delta r}{r}+2\left(1-\frac{r_p}{r}\right)\frac{\Delta V}{V}-2\tan\gamma\,\Delta\gamma$$

Now compare this equation with the one given by Chapman (ref. 2)

$$\frac{\Delta r_p}{r_p}=\frac{\Delta r}{r}+2\frac{\Delta V}{V}-2\tan\gamma\,\Delta\gamma$$

In the present analysis, variable coefficients are found for $\Delta r/r$ and $\Delta V/V$ whereas Chapman shows constant coefficients for these terms. The differences are due in part to the different set of independent variables used by Chapman (r, $\overline{V}$, and γ) and to the fact that he precluded changes in the orbit due to changes in eccentricity when he set $e=1.0$ or $\overline{V}^2=2$ prior to differentiation. The coefficient of $\Delta\gamma$, however, is the same in both equations because $\partial e/\partial\gamma=0$ for $e=1.0$.

The perigee derivatives, equations (20), (21), and (22), have been evaluated for the assumed orbits used to approximate the return lunar flight and the results are presented in figure 4. Only relatively small changes in $\partial r_p/\partial r$ are noted for the small changes in eccentricity assumed. However, the

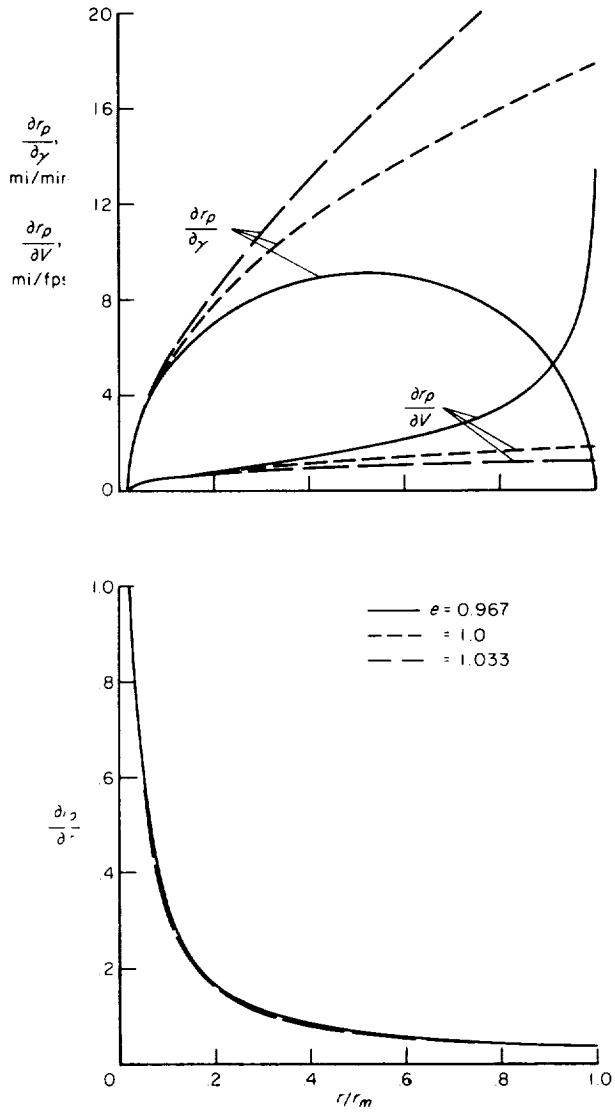

FIGURE 4.—Perigee derivatives.

converse is true for the derivatives with respect to velocity and flight-path angle, and fairly large changes in these derivatives are noted, particularly for values of range at which the vehicle is close to the moon. These derivatives, together with the calculated entry corridors, are used to evaluate guidance accuracy requirements.

OPTIMUM THRUST VECTOR FOR TRAJECTORY CONTROL

The perigee derivatives determined above may also be employed to determine the velocity increment required to correct a small error in the target perigee altitude. A change in perigee altitude due to application of thrust tangent to the flight path is given by

$$\Delta r_p=\frac{\partial r_p}{\partial V}\Delta V_t \tag{23}$$

and that due to thrust normal to the flight path is given by

$$\Delta r_p=\frac{1}{V}\frac{\partial r_p}{\partial \gamma}\Delta V_n \tag{24}$$

To determine if an optimum angle exists so that Δr_p is a maximum for a given ΔV, we assume that thrust is applied at an angle τ to the velocity vector as shown in sketch (b).

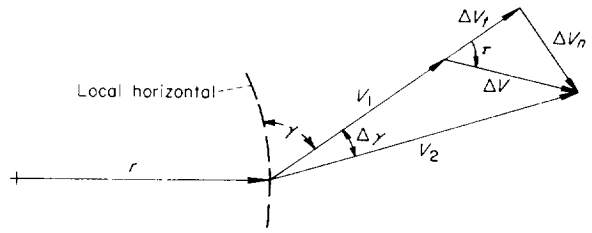

Sketch (b).

The component changes in the velocity vector are as follows:

$$\left.\begin{aligned}\Delta V_t&=\Delta V\cos\tau\\ \Delta V_n&=\Delta V\sin\tau\\ \tan\Delta\gamma&=\frac{\Delta V_n}{V_1+\Delta V_t}\end{aligned}\right\} \tag{25}$$

For small corrections, we may assume that $\Delta V\ll V$ and $\Delta\gamma\ll 1$. With these assumptions, the change in flight-path angle is approximately given by

$$\Delta\gamma=\frac{\Delta V}{V}\sin\tau \tag{26}$$

The change in perigee radius due to combined normal and tangential thrust follows from the equation for the total differential

$$\Delta r_p=\frac{\partial r_p}{\partial V}\Delta V\cos\tau+\frac{\partial r_p}{\partial\gamma}\frac{\Delta V}{V}\sin\tau \tag{27}$$

Differentiating equation (27) with respect to τ and setting $\frac{d}{d\tau}\Delta r_p=0$, we have for the thrust angle

$$\tau_{opt}=\tan^{-1}\left[\frac{(1/V)(\partial r_p/\partial\gamma)}{\partial r_p/\partial V}\right] \tag{28}$$

The second derivative, $\frac{d^2}{d\tau^2}\Delta r_p$, is negative; thus, Δr_p is a maximum for a given ΔV when the thrust is applied at the angle τ_{opt}.

With equations (21) and (22), equation (28) becomes

$$\tau_{opt}=\tan^{-1}\left[-\frac{1+e}{2}\left(\frac{1}{1-r_p/r}\right)\tan\gamma\right] \tag{29}$$

For $r\gg r_p$, the coefficient of $\tan\gamma$, $-\frac{1+e}{2}\left(\frac{1}{1-r_p/r}\right)$, is very nearly equal to -1 for the orbits considered. Thus, the optimum direction for the thrust vector is essentially along the local horizontal or normal to the range vector.

The optimum thrust or ΔV required per unit change in perigee radius is determined by setting $\tau=\tau_{opt}$ in equation (27) and rearranging thus

$$\left(\frac{\Delta V}{\Delta r_p}\right)_{opt}=\left(\frac{\partial r_p}{\partial V}\cos\tau_{opt}+\frac{1}{V}\frac{\partial r_p}{\partial\gamma}\sin\tau_{opt}\right)^{-1} \tag{30}$$

The expression for this derivative in terms of range is very simple in the case of the parabolic orbit and is easily obtained with the aid of equations (18), (21), (22), and (29) and noting that for $e=1$,

$$\cos^2\gamma=\frac{r_p}{r}\approx\cos^2(-\tau_{opt})$$

thus

$$\left(\frac{\Delta V}{\Delta r_p}\right)_{opt}\approx\frac{V_p}{2r}\left[1-\left(\frac{r_p}{r}\right)^2\right]^{-1} \tag{31}$$

RESULTS AND DISCUSSION

CORRIDOR DEPTH

The effect of L/D and G limits on entry corridor depth is presented in figure 5(a). The vacuum perigee altitude in statute miles is shown for a

vehicle with a drag loading, m/C_DA, of one slug per square foot, and the correction term for other drag loadings is indicated on the abscissa. The boundary for which exit will occur with $\overline{V}_X=1$ is given by the solid line. Above this line, for constant L/D, a vehicle will exit the atmosphere with $\overline{V}_X>1$ and multiple grazes may occur. Below the line, no exit occurs and entries are completed in the first pass. Deceleration boundaries of 10, 15, and 20 G are given by the dashed lines. (The variation with L/D of G_{max} and entrance angles for $\overline{V}_X=1$ are given in figure 5(b).

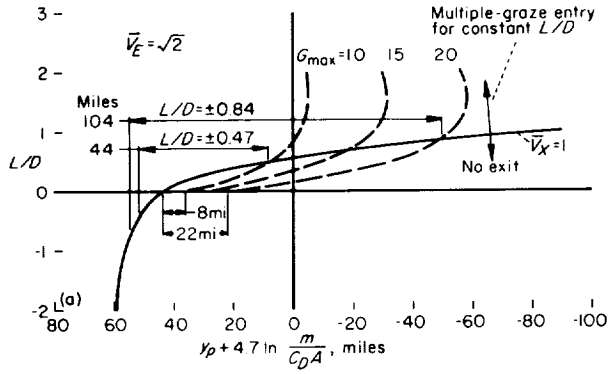

(a) Vacuum perigee.

FIGURE 5.—Entrance corridor for entry from parabolic trajectories.

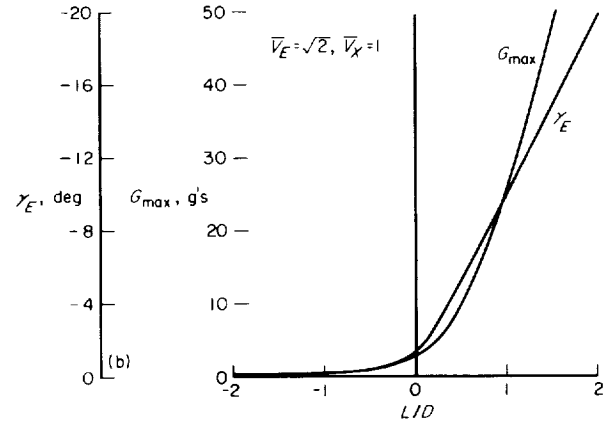

(b) Entrance angle and peak decelerations at corridor boundaries.

FIGURE 5. -Concluded.

Entrance altitudes for these angles are defined by equation (B9) in appendix B.) The depth of a corridor for a given $\pm L/D$ is, of course, dependent on the difference in drag coefficients at the L/D limits. For small L/D, the change in drag is also small and the corridor depth is essentially as given by the curves. (Note also that one of the most practical methods of obtaining a change in L/D from some positive value to some equal but negative value is simply by inversion, in which case the value of C_D is equal at corresponding values of positive and negative L/D.) It is interesting to note, then, that for small values of L/D ($L/D<1$) the amount of corridor depth gained for negative L/D is small compared to the amount gained for positive L/D although in the latter case larger decelerations are encountered. It may also be noted that for the given values of maximum G deceleration considered, lifting vehicles with $\overline{V}_X=1$ have a substantially deeper corridor, about $4\frac{1}{2}$ times deeper, than do ballistic vehicles. These results also show that for decelerations acceptable for a manned vehicle, maximum corridor depths are obtained with relatively small lift-drag ratios. For example, for 10 G, the corridor depth is a maximum of 44 miles for $L/D=\pm0.47$ and for 20 G, the corridor depth is a maximum of 104 miles for $L/D=\pm0.84$. In addition, for a given G_{max}, the use of a higher value of L/D than that which yields $\overline{V}_X=1$ would give only a small increase in corridor depth and results, of course, in $\overline{V}_X>$. In this case, multiple grazes are likely to occur with the attendant possiblity of increased radiation exposure. It might be noted here that the work of Lees (ref. 4) has indicated that the use of variable lift with constant drag can reduce the G_{max} for a given L/D at entrance. Thus for a given limiting value of G_{max}, the L/D at entrance may be increased, thus increasing the depth of the entry corridor. However, as pointed out by Chapman (ref. 6), a vehicle must fly with constant C_D as considered in Lees' analysis or with decreasing C_D (decreasing α) in order to achieve these gains in entry corridor depth. Flying the latter alternative, decreasing C_D with decreasing C_L, which will be the case unless the additional complication of variable drag devices be employed, will lead to more severe heating problems than those for a small, constant L/D.

HEATING CONSIDERATIONS

To make full use of the available entry corridor, a vehicle must be capable of operating at any $|L/D|\leq|L/D|_{max}$ and must withstand the heating associated with each L/D. The variation of heating with L/D is presented in figure 6. For the stagnation region, parameters which define

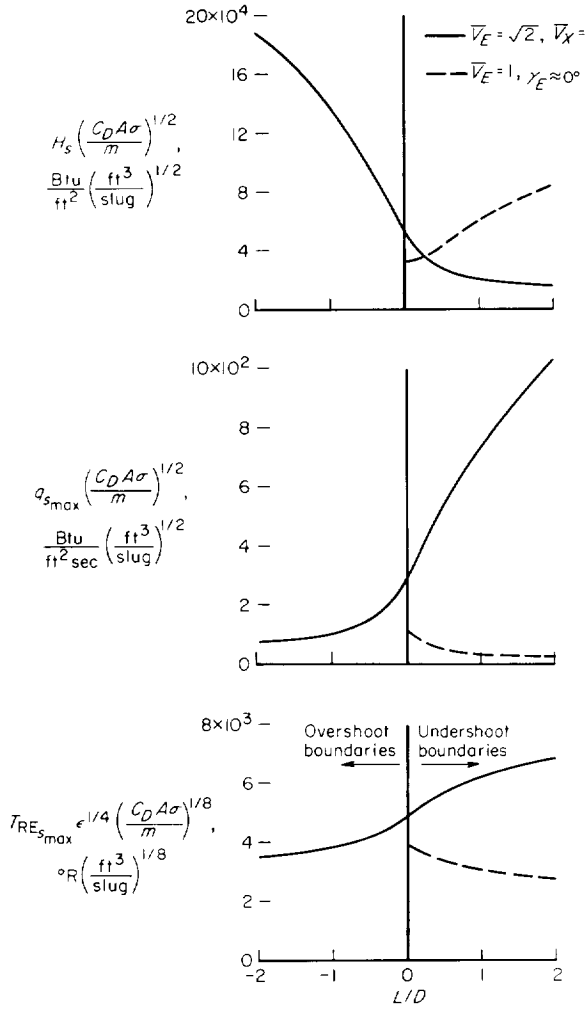

FIGURE 6.—Heating in corridor.

the maximum heating rate, unit heat-transfer load, and maximum radiation-equilibrium temperature are presented for vehicles which enter at parabolic velocity ($\overline{V}_E = \sqrt{2}$) and exit at satellite velocity ($\overline{V}_X = 1$). Corresponding curves for the satellite-entry case are shown also. For vehicles with a value of $C_D A\sigma/m$ of 1 cubic foot per slug, which appears to be a representative value, the parameters represent the actual values of maximum heating rate and heat-transfer load at the stagnation point. If the emissivity, ϵ, is also considered to be unity, then the maximum stagnation-point radiation-equilibrium temperature is also given directly by the curves. One point of interest in these results is the opposite trend of the various heating parameters with L/D in the case of parabolic graze as compared to the trend for the case of satellite entry. This difference is readily understandable when the effect of L/D on the two types of trajectories is considered. It may also be observed that for a parabolic graze, values of negative L/D are favorable for radiation-cooled vehicles because they result in lower heating rates and radiation-equilibrium temperatures, while positive values of L/D are favorable for ablation or heat-capacity cooling schemes because they result in smaller heat-transfer loads. It is apparent then that if full use of the available corridor is necessary to satisfy guidance requirements, heat shields must be capable of operating to extremes in heat-transfer load at one side of the corridor and to extremes in heating rates at the other side. Development of structure capable of radiation cooling at low heating rates and of ablation at higher heating rates appears to be one solution to this problem.

Upon closer examination of the results for the range of L/D considered, the heating parameters appear to be somewhat higher in the case of parabolic graze than in the case of satellite entry. For example, the maximum radiation-equilibrium temperature during the parabolic graze is greater than that for nonlifting satellite entry except when the lift-drag ratio is negative and greater in magnitude than unity. It is recalled from figure 5 that the corridor depth available to a vehicle restricted to this range of L/D is quite small. Since materials suitable for use with radiation-cooled nonlifting satellites are somewhat beyond present technology, the material limitations for radiation-cooled vehicles entering at parabolic velocity may further restrict the range of usable L/D and the corridor depth.

It is also recalled from figure 5 that a vehicle capable of operating over the range $-0.5 \leq L/D \leq 0.5$ in a parabolic graze has an entry corridor of reasonable depth and experiences decelerations within human tolerances. It is observed from figure 6 that for this range of L/D the heating rates are from about 1.5 to 5 times those for nonlifting-satellite entry while the unit heat-transfer load varies from about 0.9 to about 3 times as large. While these factors are large, they may still be sufficiently small for moderate values of drag loading parameters so that the ablation-type heat protection currently considered for nonlifting satellites may still be applicable for vehicles in a parabolic graze. In the end, heating considera-

tions such as these may be the deciding factors which determine the depth of the entry corridor available to a given vehicle.

VELOCITY INCREMENT FOR ORBITING AFTER INITIAL GRAZE

After an initial graze of the type being considered here, a vehicle will exit from the atmosphere with $\overline{V}_x=1$ and with a flight-path angle equal to about $-2/3$ times the entrance angle. If no action were taken, the vehicle would, of course, re-enter the atmosphere a second time. As discussed earlier, there may be occasions when it will be useful to convert the trajectory into a satellite orbit in order to better control the final descent phase of the entry. One way to accomplish such a conversion is to apply a velocity increment at the apogee of the trajectory following the initial graze. For most negative lift-drag ratios and $m/C_DA=1$, the exit angles are sufficiently small that conversion to a circular orbit at apogee following exit results in an orbit which is sufficiently low that entry would undoubtedly occur in less than one revolution. For negative lift-drag ratios, higher exit velocities or the use of positive lift near exit may be considered as methods for increasing the apogee altitude. With positive lift or for flight in the lower portions of the entry corridor, exit angles are higher and conversions to near-earth satellite orbits are possible. For example, for $L/D=0.5$ and $m/C_DA=1$, conversion to a circular orbit at an altitude of about 300 miles requires a velocity increment of about 780 fps while conversion to an eccentric orbit with a perigee at 100 miles requires about 480 fps. For the latter case, assuming a specific impulse of about 300 seconds, the weight of fuel expended is about equal to 5 percent of the vehicle weight. Again, these calculations are for constant L/D in the graze. The use of the proper lift program may greatly reduce these fuel requirements. It may also be noted that a vehicle having a sufficiently high lift-drag ratio may be capable of sufficient longitudinal and lateral range adjustment to return to a specified landing point (providing proper timing of launch from the moon can be achieved). In this case it would not be necessary to convert the trajectory to an orbit following the initial graze.

GUIDANCE ACCURACY REQUIREMENTS

With the depth of the entrance corridor known, estimates can, of course, be made of the accuracy with which a vehicle must be guided to place it within the corridor. Such estimates have been made with the use of the corridor depths taken from figure 5 and the effect of guidance errors on perigee altitude taken from figure 4. The estimates were made for several corridor depths corresponding to various combinations of L/D and maximum deceleration as shown in the following table:

G_{max}	L/D	Corridor depth, miles
10	0	8
20	0	22
10	± 0.47	44
20	± 0.84	104

The results are shown in figure 7 where the permissible errors in flight-path angle, velocity,

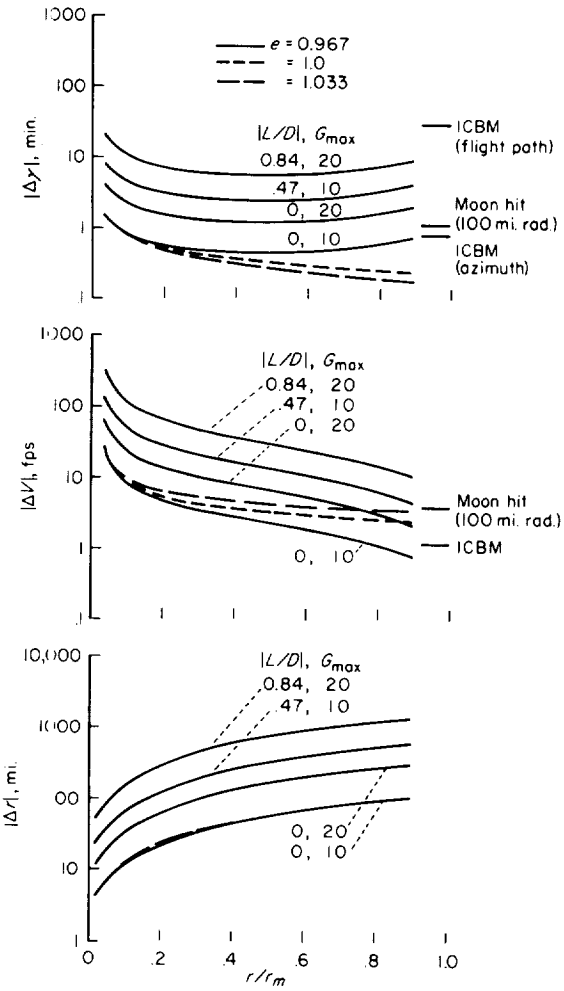

FIGURE 7.—Variation of guidance accuracy requirements with distance from the earth.

and position are presented. To obtain these results it was assumed that the vehicle was approaching the earth on the elliptic orbit discussed earlier. Since the accuracy of mid-course guidance and navigation equipment is not generally available in the literature, comparison of these permissible errors has been made with the accuracies required at the end of boost to place a vehicle on the moon within a circle of 100-mile radius (see ref. 8), and for an ICBM with the assumption of a permissible deviation of ± 1 nautical mile over a range of 5500 nautical miles.

Since the energy of the transfer trajectory may have an important effect on the accuracies required, guidance tolerances were also calculated for a ballistic vehicle experiencing a 10 G maximum deceleration (entrance corridor of 8 miles deep) for both a parabolic orbit ($e=1.0$) and a hyperbolic orbit ($e=1.033$). Permissible errors for flight-path angle, velocity, and radial position at $r/r_m=0.9$ are shown in the table below. Also shown are estimates of ICBM guidance tolerances at burnout that were obtained with the range equation for ballistic vehicles derived by Eggers, Allen, and Neice (ref. 10).

	Lunar return trajectories ($r/r_m=0.9$)			ICBM (Range=5500 ± 1 n. mi.)
	Elliptic	Parabolic	Hyperbolic	
Eccentricity	0.967	1.0	1.033	
$\Delta\gamma$, min	.736	.236	.175	29 flight path 0.8 azimuth
$\Delta V/V$	.00049	.00050	.00053	0.00005
$\Delta r/r$	.00050	.00050	.00049	0.00006

Permissible velocity and position errors are about the same for all trajectories. They are all about one order of magnitude less severe than ICBM tolerances and, therefore, do not appear critical even for the narrow corridors of ballistic vehicles. Angular accuracies required, however, are considerably more stringent than ICBM tolerances for flight-path angle. The tolerance for ICBM-azimuth angle is considerably less than that for flight-path angle and probably represents more closely the attainable limits for angular accuracies of present guidance systems. The angular accuracy requirements for the elliptical orbit come close to meeting the same requirements as for the ICBM, at least at $r/r_m=0.9$. However, from the complete results in figure 7, angular accuracy requirements for this vehicle ($L/D=0$, $G_{max}=10$) are more severe than ICBM requirements over most of the orbit. The ballistic vehicle using the elliptical orbit and a larger corridor of 22 miles and peak decelerations up to 20 g has angular tolerances which are comparable to ICBM tolerances.

In assessing these results, however, it should be recognized that mid-course navigation and guidance equipment in the near future will probably not provide the same accuracy provided by inertial systems during launch. It may be expected, therefore, that ballistic vehicles may not be suitable for the lunar flight and that the larger allowable tolerances provided by the use of lift and least energy orbits may be required to satisfy navigation and mid-course guidance requirements. It should also be noted that mid-course measurements and corrections of the velocity and position vectors to the tolerances given in figure 7 will only place the vehicle somewhere within the entry corridor. Prior to entry, a precise measurement of the location of the vehicle in the corridor must be made in order to determine the proper lift-drag ratio to be used in the graze.

OPTIMUM THRUST VECTOR FOR CORRECTION OF PERIGEE ALTITUDE

If a vehicle on its trajectory approaching the earth is sufficiently off course, it will not enter in the desired corridor. In this event, it will be necessary to alter the trajectory by the application of thrust. It is desirable to apply thrust at an angle that will produce the largest possible change in perigee altitude, for, in this manner obviously, the amount of thrust or impulse required to make a given correction will be minimized. With the aid of the equations previously developed, this optimum thrust angle, τ_{opt} (measured with respect to the local flight path), has been calculated and the results are presented in figure 8. Comparison of τ_{opt} is made with the flight-path angle, γ. For most conditions, these two angles are very nearly equal in magnitude but opposite in sign. This correspondence holds particularly at larger r/r_m and even at r/r_m of 0.1, the two angles τ_{opt} and $-\gamma$ differ by less than 4°. This finding indicates that the corrective thrust may be applied parallel to the local horizontal over most of the range with very little loss in effectiveness.

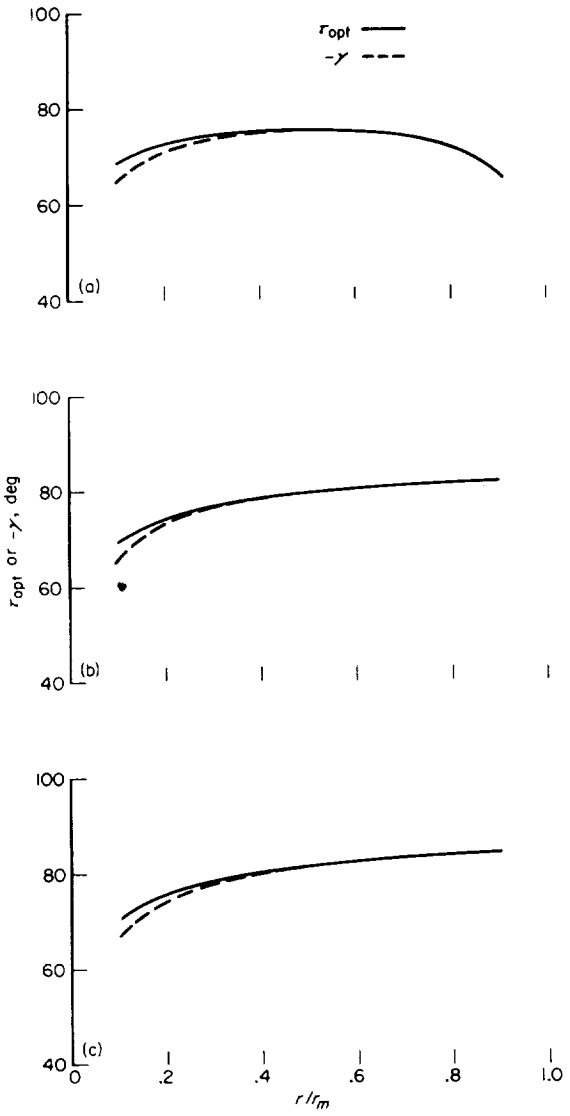

(a) $e=0.967$
(b) $e=1.0$
(c) $e=1.033$

FIGURE 8.—Optimum angle for corrective thrust impulse.

The variation with range of the increment of velocity required per unit change of perigee radius $(\Delta V/\Delta r_p)_{opt}$, is presented in figure 9. It is interesting to note that even though large variations in the derivatives, $\partial r_p/\partial V$ and $\partial r_p/\partial \gamma$, were obtained for relatively small variations in trajectory (see fig. 4), $(\Delta V/\Delta r_p)_{opt}$ is essentially the same for the three orbits considered. The explanation for this result is simply that, because of the essentially horizontal application of thrust, the change in r_p is primarily a result of changes

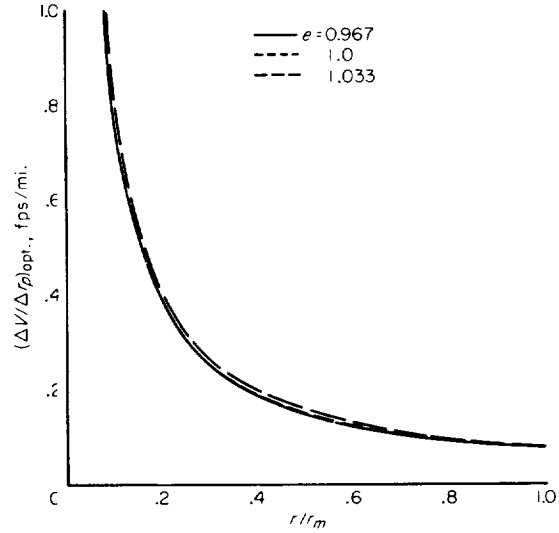

FIGURE 9.—Variation with range of increment of velocity required per mile change in perigee altitude for thrust applied at the optimum angle, $\tau=\tau_{opt}$.

in the angular momentum of the orbit. Since the angular momentum for a given r_p is proportional to the term, $\sqrt{1+e}$, the angular momentum differs little for the three orbits considered. For these reasons, the energy or ΔV required to change the orbits a given amount is essentially the same for these orbits.

Perhaps a more important point here is that the energy required to effect a given correction in perigee altitude increases with decreasing range. From equation (31) for the parabolic orbit, which from the results just presented is representative of all three orbits, the ΔV required per unit change in r_p, except near perigee, is approximately inversely proportional to the range. Thus, in order to minimize the weight penalty of fuel required, corrections should be made at the largest range possible. It is important, therefore, that the ability to detect errors accurately should extend to as large a range as practical.

CONCLUDING REMARKS

An investigation has been made to determine the effect of lift on the entrance corridor and guidance requirements for manned vehicles returning from the moon. Only strong-graze type entries in which the velocity of a vehicle is reduced to satellite speed or less in the first passage through the atmosphere were considered. Weak- or multiple-graze type entries were not considered,

as they tend to be unattractive because their guidance requirements are severe and because they expose the vehicle to the radiation belts for long periods of time.

For the purposes of this study, the entrance corridor was defined in the manner used by others as the difference in vacuum-perigee altitude of two extreme approach trajectories. These two trajectories were selected as follows: If a vehicle approached the earth on a path above the upper of the two, it would encounter insufficient air to reduce its velocity to satellite velocity and multiple grazes would result. If a vehicle approached on a path below the lower of the two extremes, it would encounter decelerations in excess of some selected maximum value.

In the study, it was found that the use of lift in amounts to produce relatively small lift to drag ratios increases the usable depth of the entrance corridor. For example, if maximum decelerations are limited to 10 g, the corridor depth increases from 8 miles for a ballistic vehicle to 44 miles for a vehicle with $L/D=\pm 0.47$. If the limit is 20 g, the depth increases from 22 miles for a ballistic vehicle to 104 miles for a vehicle with $L/D=\pm 0.84$. The use of higher lift-drag ratios is effective in further increasing the corridor depth only at the expense of higher maximum decelerations.

At the upper boundary of the corridor a vehicle encounters moderate heat-transfer rates but large total heat-transfer loads. At the lower boundary, the converse is true. For these reasons, radiation cooling appears attractive near the upper boundary and ablation cooling appears attractive near the lower boundary. If a vehicle is to make full use of its entry corridor, its structure may be required to withstand both extremes of heating. The development of structures capable of combined radiation and ablation cooling would be one solution to this problem.

Mid-course guidance requirements appear to be critical only for the flight-path angle. Increases in the energy of the transfer orbit cause increases in guidance accuracy requirements on the flight-path angle. For the least energy orbit, guidance requirements for ballistic vehicles are comparable to those for ICBM and to those for the launch of a vehicle from the earth to impact on the moon with an accuracy of ± 100 miles. Since it is unlikely that mid-course guidance and navigation equipment in the near future will provide the same degree of accuracy as inertial systems during launch, it is probable that ballistic configurations will not be suitable for the initial lunar flights of manned vehicles. Thus lifting vehicles with their increased corridor depths and associated reduced guidance requirements may be required.

To correct a trajectory for an error in vacuum perigee, it was found that application of the corrective thrust essentially parallel to the local horizontal produces the maximum change in perigee altitude for a given increment of velocity. It was also found that the energy required to effect a given change in perigee altitude is not strongly dependent on the energy of the orbit but it was found to vary inversely with range measured from the center of the earth. For this reason, it is important to detect and correct any errors in approach trajectory at the largest possible distance from the earth.

AMES RESEARCH CENTER
NATIONAL AERONAUTICS AND SPACE ADMINISTRATION
MOFFETT FIELD, CALIF., *Feb. 26, 1960*

APPENDIX A

SYMBOLS

a	semimajor axis of elliptical orbit
A	reference area, sq ft
C_D	drag coefficient, $\frac{\text{drag}}{(1/2)\rho V^2 A}$
C_L	lift coefficient, $\frac{\text{lift}}{(1/2)\rho V^2 A}$
D	drag, lb
e	Naperian logarithm base or eccentricity of orbit
f	density ratio of exponential atmosphere (see eq. (4)) and dimensionless function of reference 1, $\frac{\rho}{\rho_o \alpha}$
F	normalized f function, $\frac{f}{\sqrt{I}}$
g	gravity acceleration, 32.2 ft/sec^2
$G_{\max}$	peak resultant deceleration, g
h	angular momentum per unit mass in conic orbit, ft^2/sec
H	unit total heat transfer, Btu/ft^2
I	drag parameter, $\frac{\beta}{r_o}\left(\frac{m}{C_D A \rho_o \alpha}\right)^2$
J	lift parameter, $\frac{\sqrt{I\beta r_o}}{2}\frac{L}{D}$
$\frac{L}{D}$	lift-drag ratio
m	mass of vehicle, slugs
q	heating rate, Btu/ft^{2}sec
r	radius measured from center of earth, ft or statute miles
r_m	mean radius of moon's orbit, 1.235×10^9 ft (238,857 statute miles)
r_o	mean radius of the earth, 2.092×10^7 ft (3,963 statute miles)
t	time, sec
T_{RE}	radiation equilibrium temperature, °R
V	velocity, ft/sec
$\overline{V}$	ratio of velocity to local circular satellite speed, $\frac{V}{\sqrt{\mu/r}}$
W	vehicle weight, lb
y	altitude, feet except as noted
Z	$\ln(V^2/gr_o)$
α	constant in equation (4) of exponential atmosphere, 0.715
β	density decay parameter of exponential atmosphere, 1/24,800 ft
γ	flight-path angle measured from local horizontal, negative downward
ϵ	emissivity
θ	polar angular coordinate
λ	Stefan-Boltzmann constant, 4.81×10^{-13}, Btu/ft^{2}sec °R^4
σ	radius of curvature of stagnation region, ft
ρ	atmospheric density, slug/ft^3
ρ_o	sea-level density, 0.002378 slug/ft^3
τ	thrust angle
μ	gravitational constant for earth, 1.408×10^{16}, ft^3/sec^2

SUBSCRIPTS

a	apogee
E	entrance
ES	escape speed
opt	optimum
ov	overshoot
p	perigee
S	stagnation region
un	undershoot
X	exit

APPENDIX B

SERIES SOLUTIONS FOR MOTION AND HEATING WITHIN THE ATMOSPHERE

The methods employed to obtain the trajectories inside the atmosphere were obtained from reference 1 and they are outlined here for convenience. The transformed differential equation of motion, assuming an exponential atmosphere, is given by the expression

$$\frac{d^2f}{dZ^2}+\frac{I}{f}(1-e^{-Z})+J=0 \tag{B1}$$

where

$$f=e^{-\beta y}=\frac{\rho}{\rho_o\alpha}$$

$$Z=\ln\left(\frac{V^2}{gr_o}\right)$$

$$I=\frac{\beta}{r_o}\left(\frac{m}{C_D\rho_o A\alpha}\right)^2$$

and

$$J=\frac{\sqrt{I\beta r_o}}{2}\frac{L}{D}$$

which is subject to the restrictions of the approximations of the derivation

$$\left.\begin{aligned}&|\gamma|\ll 1\\&|W\gamma|\ll D\\&|y|\ll r_o\end{aligned}\right\} \tag{B2}$$

and assumptions of a spherical earth and fixed atmosphere.

The flight-path angle is proportional to the first derivative of f with respect to Z and is given by

$$\gamma=\frac{1}{\sqrt{\beta r_o I}}\frac{df}{dZ}\equiv\frac{F'}{\sqrt{\beta r_o}} \tag{B3}$$

Equation (B1) may be rearranged as follows:

$$\frac{d^2f}{dZ^2}+\frac{Ie^{-Z_o}}{f}[e^{Z_o}-e^{-(Z-Z_o)}]+J=0 \tag{B4}$$

A series solution to equation (B4) for grazing entries was given in reference 1 as

$$\frac{f}{\sqrt{Ie^{-Z_o}}}\equiv\frac{F}{e^{-Z_o/2}}=\sum_{i=0}^{n}k_i(Z-Z_o)^i \tag{B5}$$

The constants for this solution were obtained (in ref. 1) by substitution of equation (B5) and a series expansion for $e^{-(Z-Z_o)}$ in equation (B4) and by application of the boundary condition, $F'=0$ at $Z=Z_o$; terms having like powers of $Z-Z_o$ were collected and the coefficients equated to zero. Solutions of the equations obtained yield for the coefficients of equation (B5)

$$k_1=0$$

$$k_2=-\frac{1}{2k_o}\left(e^{Z_o}-1+\frac{k_o}{2}\sqrt{\beta r_o}e^{Z_o}\frac{L}{D}\right)$$

$$k_3=-\frac{1}{6k_o}$$

It may be noted that since only one of the two required boundary conditions has been applied, all subsequent coefficients occur in terms of k_o. For grazes having exit velocities not lower than local circular satellite speed, it is sufficient to retain terms up to and including $(Z-Z_o)^2$, thus

$$\frac{f}{\sqrt{I}}\equiv F=k_oe^{-Z_o/2}\left[1-\frac{1}{2k_o^2}\left(e^{Z_o}-1+\frac{k_o}{2}\sqrt{\beta r_oe^{Z_o}}\frac{L}{D}\right)(Z-Z_o)^2\right] \tag{B6}$$

where k_o is determined from the boundary condition that $F=0$ at $Z=Z_{ES}=\ln 2$ which yields the following quadratic for k_o

$$k_o^2-\frac{k_o}{4}\sqrt{\beta r_oe^{Z_o}}\left(\frac{L}{D}\right)(Z_{ES}-Z_o)^2-\frac{e^{Z_o}-1}{2}(Z_{ES}-Z_o)^2=0 \tag{B7}$$

It may also be noted that for $F=0$ at $Z=Z_{ES}$ the coefficient of $(Z-Z_o)^2$ in equation (B6) is equal to $1/(Z_{ES}-Z_o)^2$. For exit ($F=0$), at satellite speed, Z_o in equation (B6) is $Z_{ES}/2$; and for exit above satellite speed, $Z_o=(Z_{ES}+Z_X)/2$.

The boundary conditions, $F=0$ at $Z=Z_{ES}$ or Z_X, place the initial and final ends of the trajectory

at $y=\infty$. While applying the boundary conditions at ∞ has only a small effect on the motion and heating in the lower portions of the trajectory, motion near the initial and final portions of the trajectory is not adequately described by the solution, nor, in fact, by the differential equation (eq. (B4)). Equation (B4) and its solutions are, of course, subject to the restrictions of condition (B2). We may, therefore, apply these conditions to determine the altitudes at which the equations first become valid on entry and cease to be valid at exit. In general, the third inequality of condition (B2) is less restrictive than the second and it is usually satisfied when the second inequality is met. The second inequality states that the analysis is valid when the weight component along the flight path is small compared to the drag force. This condition is satisfied at entrance and exit by $|mg\gamma|=0.1D$ which in terms of the F functions is

$$\left|\frac{F'}{F}\right|=\frac{\beta r_o e^Z}{20} \tag{B8}$$

Equation (B8) was used to relate F and F' of the entrance and exit conditions for the machine solutions. For the series solutions, boundary conditions were applied as given and entrance and exit parameters determined as follows:

1. An approximate evaluation of equation (B8) is obtained first by setting $Z_E=Z_{ES}$ and $Z_X=0$, thus

$$F_E=-\frac{10}{\beta r_o}F_E' \text{ and } F_X=\frac{20}{\beta r_o}F_X' \tag{B9}$$

2. With the use of equation (B6) and its first derivative, equations (B9) become quadratics in $(Z-Z_o)$ which are easily solved for the values of Z at entrance and exit. By substitution of these values of Z_E and Z_X in equation (B6), entrance and exit parameters are obtained which satisfy conditions (B2) and are given by

$$\left.\begin{aligned} &F_E=C_E F_o=C_E k_o e^{-Z_o/2} \\ \text{and}\quad &F_X=C_X F_o=C_E k_o e^{-Z_o/2} \\ \text{where}\quad &C_E=\left[1-\left(\frac{Z_E-Z_{ES}/2}{Z_{ES}/2}\right)^2\right]=0.066 \\ &C_X=\left[1-\left(\frac{Z_X-Z_{ES}/2}{Z_{ES}/2}\right)^2\right]=0.088 \end{aligned}\right\} \tag{B10}$$

The peak resultant deceleration occurs near the minimum altitude point in the graze and is approximately given by

$$G_{\max}=\sqrt{\beta r_o}\,\frac{k_o e^{Z_o/2}}{2}\sqrt{1+\left(\frac{L}{D}\right)^2} \tag{B11}$$

The stagnation-region heating rate is given by

$$q_S=K_1\sqrt{k_o}\,e^{5Z_o/4}\left[1-\left(\frac{Z-Z_o}{Z_{ES}-Z_o}\right)^2\right]^{1/2} e^{(3/2)(Z-Z_o)} \tag{B12}$$

where

$$K_1=\frac{C_S}{778}(gr_o)^{3/2}\left(\frac{\beta}{r_o}\right)^{1/4}\left(\frac{m}{C_D A\sigma}\right)^{1/2}$$

and

$$C_S=1.67\times10^{-5}, \sqrt{\text{slug}}/\text{ft} \qquad \text{(see ref. 11)}$$

and peak heating occurs at

$$(Z-Z_o)q_{S_{\max}}=-\frac{1}{3}+\frac{1}{3}\sqrt{1+9(Z_{ES}-Z_o)^2}$$

The unit heat-transfer load to the stagnation region, assuming a cold wall and laminar-continuum flow, is given by

$$H_S=K_2\frac{\pi e^{5Z_o/4}}{\sqrt{k_o}}(Z_{ES}-Z_o) \tag{B13}$$

where

$$K_2=\frac{C_S}{778}gr_o\left(\frac{r_o}{\beta}\right)^{1/4}\left(\frac{m}{C_D A\sigma}\right)^{1/2}$$

The stagnation-region radiation-equilibrium temperatures follow from equation (B12) and the Stefan-Boltzmann law, thus

$$T_{RE_S}=\left(\frac{q_S}{\epsilon\lambda}\right)^{1/4} \tag{B14}$$

where ϵ is the emissivity and λ is the Stefan-Boltzmann constant.

REFERENCES

1. Eggers, Alfred J., Jr.: The Possibility of a Safe Landing. Space Technology, ch. 13, Howard S. Seifert, ed., John Wiley and Sons, Inc., 1959, pp. 13-01 to 13-53.
2. Chapman, Dean R.: An Approximate Analytical Method for Studying Entry Into Planetary Atmospheres. NASA Rep. 11, 1959. (Supersedes NACA TN 4276)

3. Gazley, Carl, Jr.: Deceleration and Heating of a Body Entering a Planetary Atmosphere From Space. Rand Rep. P–955, 1957.

4. Lees, Lester, Hartwig, Frederic W., and Cohen, Clarence B.: The Use of Aerodynamic Lift During Entry Into the Earth's Atmosphere. Rep. GM–TR–0165–00519, Space Technology Lab., Nov. 1958.

5. Xenakis, George: Some Flight Control Problems of a Circumnavigating Lunar Vehicle. WADC TN 58–82, 1958.

6. Chapman, Dean R.: An Analysis of the Corridor and Guidance Requirements for Supercircular Entry Into Planetary Atmospheres. NASA TR R–55, 1960. (Supersedes NASA TN D–136)

7. Van Allen, James A.: Radiation Belts Around the Earth. Scientific American, v. 200, no. 3, March 1959, pp. 39–47.

8. Lieske, H. A.: Accuracy Requirements for Trajectories in the Earth-Moon System. Rand Rep. P–1022, 1957.

9. Moulton, Forest Ray: An Introduction to Celestial Mechanics. The Macmillan Co., 1914.

10. Eggers, Alfred J., Jr., Allen, H. Julian, and Neice, Stanford E.: A Comparative Analysis of the Performance of Long-Range Hypervelocity Vehicles. NACA TN 4046, 1957.

11. Eggers, Alfred J., Jr., Hansen, C. Frederick, and Cunningham, Bernard E.: Stagnation-Point Heat Transfer to Blunt Shapes in Hypersonic Flight, Including Effects of Yaw. NACA TN 4229, 1958.

U. S. GOVERNMENT PRINTING OFFICE: 1961